THE JOURNAL OF PHYSICAL CHEMISTRY B
A JOURNAL OF THE AMERICAN CHEMICAL SOCIETY

pubs.acs.org/JPCB

Article

How Water–Ion Interactions Control the Formation of Hydrated Electron:Sodium Cation Contact Pairs

Published as part of The Journal of Physical Chemistry virtual special issue "Dor Ben-Amotz Festschrift".

Sanghyun J. Park, Wilberth A. Narvaez, and Benjamin J. Schwartz*

Cite This: *J. Phys. Chem. B* 2021, 125, 13027–13040

Read Online

ABSTRACT: Although solvated electrons are a perennial subject of interest, relatively little attention has been paid to the way they behave in aqueous electrolytes. Experimentally, it is known that the hydrated electron's (e_{aq}^-) absorption spectrum shifts to the blue in the presence of salts, and the magnitude of the shift depends on the ion concentration and the identities of both the cation and anion. Does the blue-shift result from some type of dielectric effect from the bulk electrolyte, or are there specific interactions between the hydrated electron and ions in solution? Previous work has suggested that e_{aq}^- forms contact pairs with aqueous ions such as Na^+, leading to the question of what controls the stability of such contact pairs and their possible connection to the observed spectroscopy. In this work, we use mixed quantum/classical simulations to examine the nature of Na^+:e^- contact pairs in water, using a novel method for quantum umbrella sampling to construct e_{aq}^-–ion potentials of mean force (PMF). We find that the nature of the contact pair PMF depends sensitively on the choice of the classical interactions used to describe the Na^+–water interactions. When the ion–water interactions are slightly stronger, the corresponding cation:e^- contact pairs form at longer distances and become free energetically less stable. We show that this is because there is a delicate balance between solvation of the cation, solvation of e_{aq}^- and the direct electronic interaction between the cation and the electron, so that small changes in this balance lead to large changes in the formation and stability of e^-–ion contact pairs. In particular, strengthening the ion–water interactions helps to maintain a favorable local solvation environment around Na^+, which in turn forces water molecules in the first solvation shell of the cation to be unfavorably oriented toward the electron in a contact pair; stronger solvation of the cation also reduces the electronic overlap of e_{aq}^- with Na^+. We also find that the calculated spectra of different models of Na^+:e^- contact pairs do not shift monotonically with cation–electron distance, and that the calculated spectral shifts are about an order of magnitude larger than experiment, suggesting that isolated contact pairs are not the sole explanation for the blue-shift of the hydrated electron's spectrum in the presence of electrolytes.

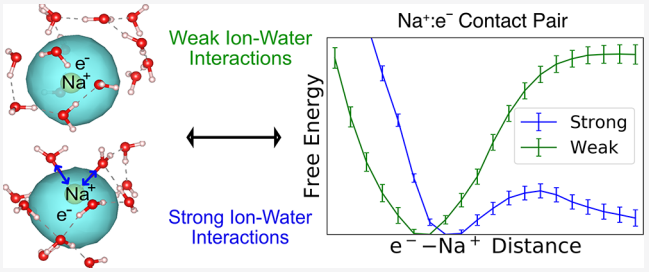

INTRODUCTION

When an excess electron is introduced into liquid water, the resulting solvated object is known as a hydrated electron. Despite the importance of the hydrated electron in many fields, especially radiation chemistry,[1,2] there is still not a unifying underlying picture that can explain all of its properties, such as the temperature dependence of the electron's absorption spectrum[3−7] and EPR *g*-factor,[8−11] the fact that the electron's molar solvation volume does not appear to be temperature dependent[11,12] but the radius of gyration from spectral moment analysis does,[13] etc. One particularly interesting feature of the hydrated electron that has received somewhat less attention is that its properties also depend on whether or not there are other ions present in the aqueous solution. Experimental work by Mostafavi and co-workers demonstrated that the steady-state absorption spectrum of the hydrated electron blue shifts in the presence of electrolytes.[14,15] The magnitude of the blue shift depends on the concentration of the electrolyte and the identities of not only the salt cation but also the anion.

Although the experimental observation of how the spectrum of the hydrated electron changes in the presence of electrolytes was presented over 15 years ago, there have been only limited attempts to understand the origins of the salt-dependent shifts from a theoretical perspective.[16,17] Although much of the recent efforts in the literature are focused on performing *ab initio* simulations of the hydrated electron,[18−24] computational expense limits such calculations to at most a few tens of water

Received: September 19, 2021
Revised: October 26, 2021
Published: November 22, 2021

https://doi.org/10.1021/acs.jpcb.1c08256
J. Phys. Chem. B 2021, 125, 13027–13040

molecules and a few tens of picoseconds of dynamics. This means that *ab initio* simulation of an aqueous system with a high concentration of electrolytes and an excess electron is prohibitively expensive: the number of atoms needed is well into the hundreds, and capturing the slow diffusive motions of the ions is simply out of reach, even with relatively inexpensive methods such as DFT. Thus, with current technology, this is a question that can only be addressed by approximate methods.

The main theoretical effort in area of hydrated electrons in aqueous electrolytes to date comes from Boutin and co-workers, who examined the potential of mean force (PMF) between a single Na^+ cation and a hydrated electron.[16,17,25] These researchers used mixed quantum/classical (MQC) molecular dynamics (MD) simulations, where the water molecules and sodium cation were treated classically and the quantum-mechanically treated electron interacted with the classical particles via pseudopotentials. Even with this level of theory, calculating an electron−ion PMF is challenging because the ability to restrain the distance between a quantum electron and a classical sodium cation requires evaluating forces on all of the water molecules that determine precisely where the hydrated electron's center-of-mass is located. Boutin and co-workers accomplished this with a perturbation-theory-based method,[26] and they found that the PMF consists of a well that is ∼5 k_BT deep with an energetic minimum located at an e^-−Na^+ distance of ∼2 Å: in other words, they found that Na^+ forms a stable contact pair with the hydrated electron.[17]

Boutin and co-workers then went on to examine how the absorption spectrum of the MQC-simulated hydrated electron varies as a function of distance from the Na^+ cation. They found that proximity to a sodium cation indeed led to a blue-shift of the electron's calculated spectrum and that the magnitude of the spectral shift varied roughly inversely with the sodium−electron distance.[17] This suggested that the blue-shift of the hydrated electron's spectrum is largely due to the electrostatic interaction between the cation and the electron and that chemical interactions (i.e., orbital overlap) between the electron and sodium cation or an altering of the local solvation structure of around the hydrated electron when it is in the proximity of the cation play less important roles.

For all of the success of the MQC model in explaining the spectral blue-shift of hydrated electrons in aqueous electrolytes, the simulations still failed to capture many aspects of the experiment. First, the calculated blue-shifts[17] were significantly larger than those observed experimentally.[14] In addition, the experiments found that although the spectrum of the hydrated electron blue-shifted in the presence of salts, the shape of the spectrum remained invariant.[14] Boutin and co-workers' MQC simulations, however, found that the hydrated electron's spectrum changed shape quite a bit when in a contact pair with a sodium cation.[15,17] Finally, when Boutin and co-workers attempted to mimic the concentration dependence of the electron's spectrum by varying the electron−cation distance,[17] the spectral behavior had a different dependence than that seen experimentally.[14]

These discrepancies mean that something in the MQC simulations is not capturing the correct experimental behavior. The differences could be because the simulations looked at only a single cation rather than a high concentration of neutral salt consisting of multiple cations and anions. They also could arise because one of the interactions in the simulation is not properly tuned to correctly understand the properties of the system. The interactions include the pseudopotential between the electron and water, for which Boutin and co-workers chose the Turi−Borgis (TB) potential, which yields a hydrated electron in a well-defined cavity in the water.[27−30] The simulations also include a pseudopotential between the electron and sodium cation,[31,32] as well as classical interactions of the water molecules with each other and with the sodium cation.[33] This leads to the central question addressed in this work: presuming that the MQC level of theory is sufficient to draw insights into this system, which interactions are most important in determining the behavior of hydrated electrons in the presence of aqueous electrolytes?

In this paper, we revisit MQC simulations of a hydrated electron interacting with a single sodium cation in liquid water. We explore the PMF between a hydrated electron and a sodium cation using a new method for quantum umbrella sampling.[34] Although *ab initio* methods have provided some success in reproducing the experimental features associated with the hydrated electron,[18,24] performing umbrella sampling with *ab initio* methods is currently not feasible: even with DFT, the computational cost of running numerous trajectories at different values of the umbrella parameter is prohibitive, and as of yet, there has been no quantum umbrella sampling method that works with *ab initio* generated wave functions or spin densities. This is why we focus on using MQC simulations to generate hydrated electron:sodium cation PMFs to explore how the interplay between the quantum and classical interactions affect the formation of the contact pair and the blue shift of the absorption spectrum. Although the accuracy of the MQC simulation is inferior to *ab initio* calculations, MQC simulations still successfully capture most of the features observed experimentally, including the blue-shift of the electron's absorption spectrum from the addition of cations.

Here, we specifically explore how changing the classical interactions between the water and the sodium cation, leaving all the pseudopotentials and the water−water interactions constant, affects the PMF governing e^-:Na^+ contact pairs. We find that sodium cation−hydrated electron contact pair stability is heavily affected by the choice of classical Na^+-water interaction. We show that contact pair stability is determined by a subtle balance between the classical and quantum interactions, including electron solvation, cation solvation, and the cation−electron attraction. We find that even a slight tipping of this balance can lead to dramatic changes in the way hydrated electrons behave in the presence of electrolytes. Stronger cation−water interactions lead to more unfavorable solvation structures and thus a net destabilization of Na^+:e^- contact pairs. Thus, to properly simulate objects like cation:electron contact pairs, it is important to correctly describe the classical solvation of the ion as well as the quantum mechanics of the solvated electron.

METHODS

To investigate the role that classical cation−water interactions play in the properties of hydrated electron:cation contact pairs, we used MQC MD simulations. The methods we use closely follow our previous work simulating the hydrated electron, as well as the work of Boutin and co-workers.[17,30,34] Our simulation box contained 497 classical SPC/flex water molecules,[35] one classical Na^+ cation, and a quantum mechanically treated electron. The dynamics were run in the canonical (N, V, T) ensemble. The wave function of the excess electron was represented in a basis of 24 × 24 × 24 grid points centered in the simulation box. Following the work of Boutin

https://doi.org/10.1021/acs.jpcb.1c08256
J. Phys. Chem. B 2021, 125, 13027−13040

and co-workers, we used the TB pseudopotential to treat the electron-water interactions.[27,28] We used our previously developed pseudopotential to represent the electron−Na^+ interaction.[31,32] The classical subsystem was propagated using the velocity Verlet algorithm with a 0.5 fs time step,[36] and forces from the quantum mechanical electron were evaluated every time step via the Hellman−Feynman theorem.[37] The system density was fixed at 0.997 g/cm^3, and the temperature was held constant at 298 K using the Nose−Hoover chain thermostat.[38]

The main thrust of this study is to examine the effects of choosing different classical Na^+−water interactions on the properties of the MQC system. We thus explored three different sets of parameters representing the interactions between the classical sodium cation and the flexible SPC water. The first set of Na^+−O parameters is taken from work by Dang et al., who chose the Lennard-Jones (LJ) parameters for this interaction by fitting them to match the experimental enthalpy of gas-phase ion−water clusters.[39] The second set of water−ion parameters is taken from Koneshan et al.,[40] who refitted an earlier potential due to Pettitt and Rossky[41] into the Lennard-Jones form. Finally, the third set of cation-water LJ parameters were taken from the work of Aqvist et al., who adjusted the parameter values to reproduce the experimental $\Delta G_{hydration}$ of different ions.[42] All three sets of parameters are summarized in Table 1.

Table 1. Na^+−Water Oxygen Lennard-Jones Parameters Used in This Work[a]

	Dang[39]	Koneshan[40]	Aqvist[42]
σ_{Na-O} (Å)	2.758	2.728	3.247
ϵ_{Na-O} (kJ/mol)	0.595	0.560	0.086

[a]The Aqvist parameters show the largest ion radius with shallowest energy well. The Dang and Koneshan parameters are similar with Koneshan showing the smallest ion and Dang showing the deepest energy well.

Even though these sets of parameters are designed to simulate the same system—a sodium cation in liquid water—the sets of parameters are noticeably different as they were optimized using different targets. The Aqvist parameters have the largest sodium size with a shallow energy well. This implies that the sodium−water interactions that are relatively weak compared to the other parameter sets. The Dang and Koneshan parameters look more similar to each other, but do have minor differences; the Dang parameters have the deepest energy well while the Koneshan parameters yield the smallest sodium cation size.

The principal focus of this work is to see how different ion−water interactions affect the potential of mean force (PMF) between the hydrated electron and the cation. To do this, the distance between the electron's center-of-mass and the sodium cation needs to be restrained so that the free energy can be calculated. Although this is standardly done by umbrella sampling in all-classical simulations, it is not straightforward to extend umbrella sampling to quantum mechanical particles because the quantum Hamiltonian does not commute with the umbrella potential.[26] To circumvent this problem, the umbrella potential can instead be applied to an expectation value of the quantum subsystem, so that the quantum degree of freedom is integrated out. In our case, this will be the expectation value of the electron's position, or center-of-mass.

The difficulty with restraining quantum expectation values in MQC simulations is that the forces that restrain the quantum expectation value have derivative terms that involve how the expectation value changes with motion along each of the classical coordinates. Borgis and co-workers used a perturbation-theory approach to evaluate these derivatives, a method referred to as sum-over-states quantum umbrella sampling (SOS-QUMB).[26] This method has the advantage that it can be relatively inexpensive to calculate the required forces but has the disadvantage that it is only exact when all possible quantum eigenstates are incorporated into the calculation, and the convergence properties when truncating the sum are unknown. Thus, in this work, we take advantage of a method that we previously developed that evaluates the necessary derivatives by using the coupled-perturbed response equations.[34] Although somewhat more expensive than calculating only a few terms of the SOS-QUMB expansion, the coupled-perturbed quantum umbrella sampling (CP-QUMB) method can evaluate the exact forces on the classical coordinates needed to restrain a quantum expectation value. In previous work, we have successfully applied CP-QUMB to restrain the position of a hydrated electron relative to the air/water interface[43] and also to restrain the number of water molecules within a given distance of the hydrated electron's center of mass,[44] so we use this method for all of the calculations described below.

To calculate PMFs for each set of ion−water LJ interaction parameters, we first employed 15 simulation windows for differently restrained electron−ion distances: one every 0.25 Å, starting from 0 Å separation to 4 Å separation of the Na^+−e^- center-of-mass distance. For electron−ion distances beyond 4 Å, it appeared that the PMFs had largely reached their asymptotes, so we only ran three additional simulation windows separated by 0.5 Å. The restraining harmonic umbrella potential had a force constant of 1.5 eV/$Å^2$ in all our simulation windows. With this choice of the umbrella force constant, we found good overlap of the distributions for neighboring simulation windows, providing good statistics for constructing the PMF by connecting the data from each window using the multistate Bennett acceptance ratio method,[45] as described in more detail in the Supporting Information. Each simulation window was run for at least 25 ps, truncating the first 5 ps to ensure equilibrium. For the remaining 20 ps of data, uncorrelated configurations were drawn every 200 fs and used for data analysis.

RESULTS AND DISCUSSION

Effect of Changing Ion−Water Interactions on Na^+−e^- Potentials of Mean Force. We begin our exploration of the effects of the role of cation−water interactions in determining how hydrated electrons interact with sodium cations by examining the cation−electron PMFs, calculated from the CP-QUMB method; the PMFs are shown in Figure 1a. It is worth emphasizing that, for these simulations, all interactions—the water−water, electron−water and electron−sodium interactions—are identical and that the only difference between them is the choice of LJ parameters representing the Na^+−water interaction. Clearly, the choice of ion−water interaction makes a significant difference in the way the ions interact with the hydrated electron. In particular, although all three PMFs suggest that the electron does form a stable contact pair with the sodium cation, each PMF shows a different well depth and optimal distance for the contact pair.

https://doi.org/10.1021/acs.jpcb.1c08256
J. Phys. Chem. B 2021, 125, 13027−13040

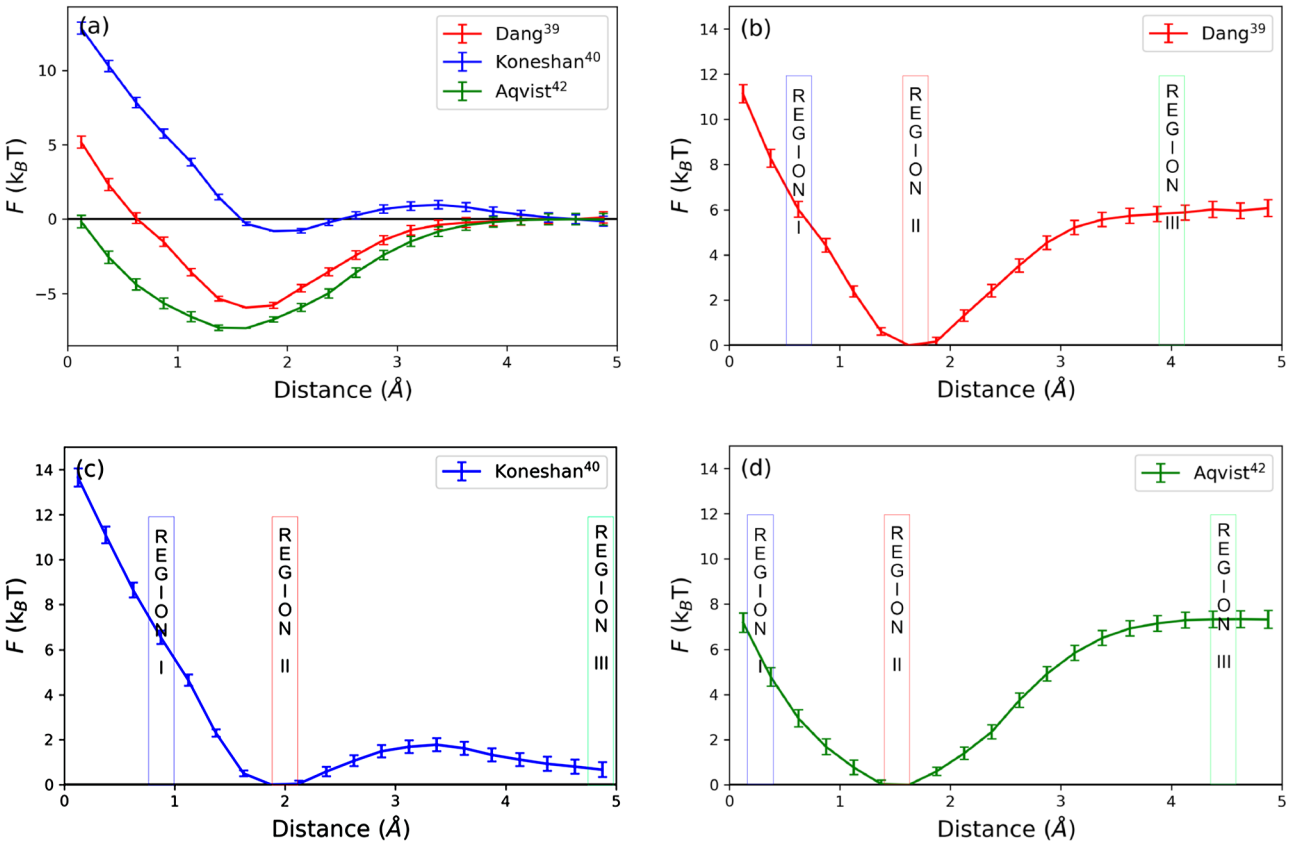

Figure 1. (a) Hydrated electron–Na^+ PMFs calculated using the CP-QUMB method with the TB model of the electron and identical simulation parameters except for the LJ parameters describing the water–Na^+ interaction, taken from the models of Dang et al. (red curve), Koneshan et al. (blue curve), and Aqvist et al. (green curve). All three PMFs show a free-energy minimum in the region between 1.5–2.0 Å, indicating that hydrated electrons form stable contact pairs with sodium cations. The three curves show remarkably different contact-pair stabilities, however, indicating that the ion–water interactions are important in determining the behavior of electron–ion contact pairs. (b–d) Same PMFs shown in panel a, with the three regions chosen for further analysis (6 k_BT above the free-energy minimum, the free-energy minimum, and the region along the long-distance asymptote) marked; the three regions occur at slightly different distances for each model because of the differences in the PMFs.

The Aqvist LJ parameters (green curve) produce a PMF with the deepest well (~8 k_BT) and the shortest equilibrium distance between the Na^+ and the center of the hydrated electron. The Koneshan sodium-cation–water LJ parameters (blue curve), on the other hand, yield an electron–cation PMF with a shallow well that has only ~2 k_BT stability relative to the energetic maximum at 3.5 Å separation, indicating a contact pair that is barely stable relative to free ions. Finally, the Dang ion–water LJ parameters (red curve) lead to an intermediate PMF, with a ~6 k_BT well depth and an intermediate distance for the equilibrium separation.

We note that the previous work by Boutin and co-workers also used the Aqvist LJ parameters to describe the Na^+–water interaction, and the other interactions in their simulations were also similar to ours except for the quantum umbrella sampling method. Boutin and co-workers indeed observed features in their calculated PMF that are similar to those generated in our work, with a ~6k_BT deep free energy well whose minimum was at an electron center-of-mass to cation distance of ~1.75 Å. At longer distances, however, the PMF by Boutin and co-workers showed a significant decrease in free energy, and the asymptotic region was not reached until distances of ~9 Å. We note that Boutin and co-workers did not show error bars on their calculated PMF, so it is unclear if the barrier they observe and long-distance PMF falloff is within the calculated error, or possibly might be a result of a convergence failure of the SOS-QUMB method they employed at longer distances.

The general features of the PMFs for the three models that we observe in Figure 1a can be rationalized as follows. As the electron–ion distance approaches zero, the excess electron is forced to be centered on the sodium cation, so the system behaves effectively as a solvated neutral sodium atom. Neutral sodium atoms have the largest possible electronic stability, but they are also hydrophobic objects, and thus there is a net free-energy penalty to solvate them in liquid water. At long electron–ion distances, the Na^+ and hydrated electron are solvated separately with minimal electronic interaction, defining the zero of free energy. Finally, at intermediate electron–ion distances, there is some favorable electronic interaction between the electron and the sodium, and the partially separated species, which has a significant dipole moment, is also reasonably well solvated, leading to stable contact-pair formation.

The presence and stability of electron–cation contact pairs is of critical importance in radiation chemistry, electrochemistry and other fields,[46−49] but the results in Figure 1 suggest that without careful consideration of how the ions interact with the water, we are not able to have a good theoretical understanding of how such ions interact with excess electrons. Thus, the questions that form the focus of the remainder of this paper are why do relatively minor changes in

https://doi.org/10.1021/acs.jpcb.1c08256
J. Phys. Chem. B 2021, 125, 13027−13040

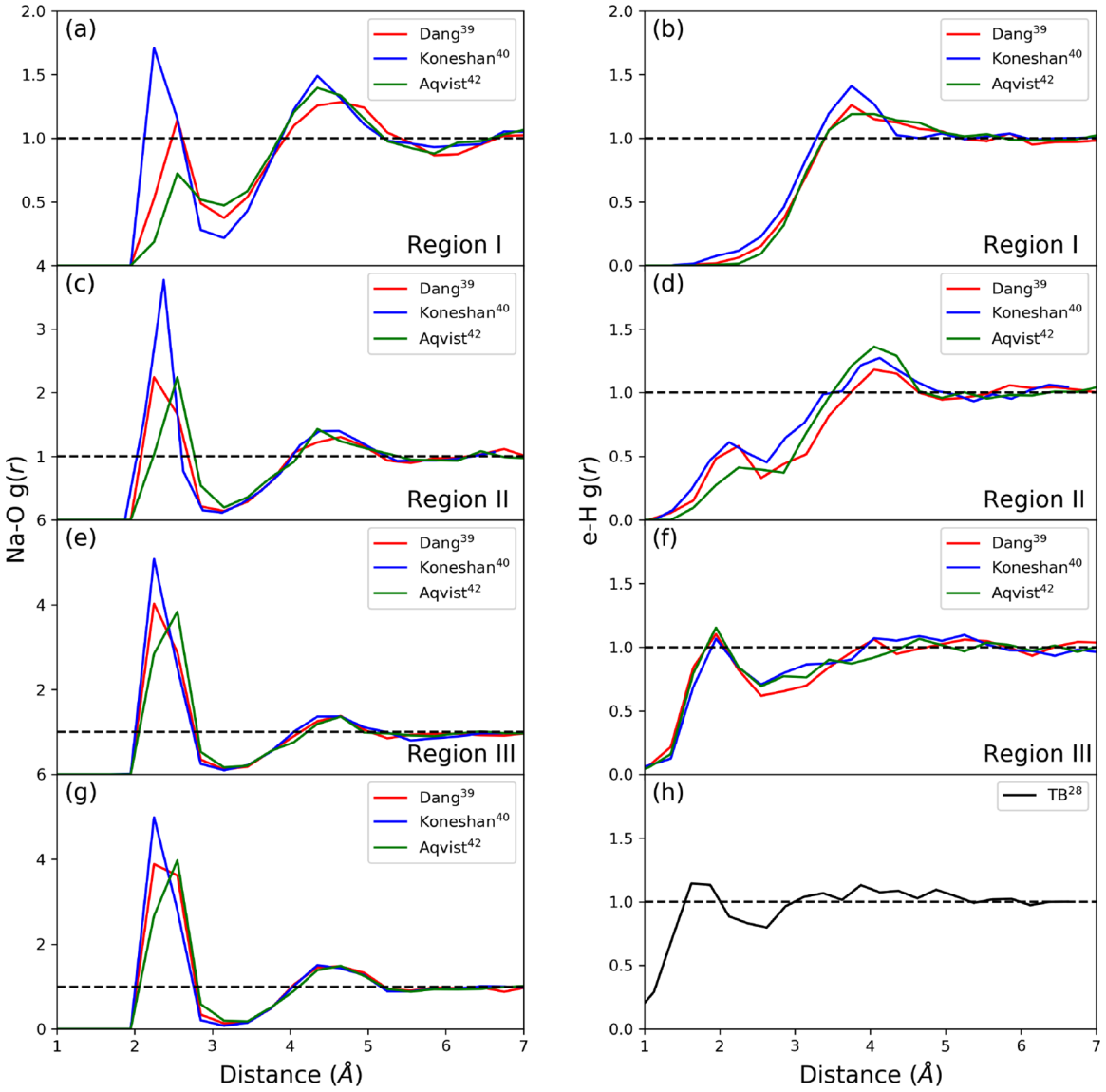

Figure 2. Radial distribution functions showing the probability to find water O atoms as a function of distance from the Na^+ (left column) and to find water H atoms from the center-of-mass of the hydrated electron (right column) for the three different models in each of the three regions delineated in Figure 1. The colors of each curve represent the model used, the same is in Figure 1, and the first, second and third row of panels show the behavior in regions I, II, and III, respectively. The bottom row shows the solvation structure for the isolated systems with only a Na^+ or a hydrated electron. As the Na^+–e^- distance reaches the PMF asymptote in region III, the solvation structures of both the electron and cation approach those of the isolated species. As the sodium cation is restrained to reside closer to the electron's center of mass, regions I and II, the solvation of the electron is strongly affected: the number of first-shell H atoms decreases dramatically, and a new e^--H peak appears at further distances. The number of first-shell waters around the cation (note the change in the *y*-axis scale between the different panels showing the Na^+–O distributions) also decreases as the cation is forced toward the electron's center. The Koneshan model Na^+ (blue curves), which has the strongest ion–water interaction, retains the most first-shell waters as the electron approaches, some of which are then forced to be in the first shell of the hydrated electron.

the water–Na^+ interactions make such dramatic changes to contact pair formation between the sodium cation and hydrated electron? What type of trade-off is there between hydrated electron solvation, cation solvation and electron–cation interactions that yields such vastly different behaviors with relatively subtle changes in the interactions? Can we compare the calculated properties of the different simulated cation–electron contact pairs to experiment?

To answer these questions, we examine the properties of the different simulated e^-:Na^+ contact pairs in three different regions of their respective PMFs. Region I is chosen to be at electron–ion distances shorter than the contact-pair equilibrium distance at a free energy 6 k_BT above the minimum. Region II is chosen to be at the contact-pair free-energy minimum for each model, and region III is chosen at large electron–ion distances along the PMF asymptote. Because the PMFs for each model are so different, the precise electron–ion distances for each region are also different, as shown explicitly for each model in Figure 1b–d. One interesting feature in the Koneshan PMF is that there is a maximum at 3.5 Å making it difficult to determine the asymptotic region. Thus, for this model, we chose region III at the farthest distance we calculated as the best representation of asymptotic behavior.

https://doi.org/10.1021/acs.jpcb.1c08256
J. Phys. Chem. B 2021, 125, 13027–13040

Solvation Structure of Hydrated Electron−Na^+ Contact Pairs. We begin our analysis of the three different simulation models by examining the solvation structures of the electron and sodium cation at different electron−ion distances. Figure 2 plots e^-−H (right side) and Na^+−O (left side) radial distribution functions, $g(r)$, for all three models in each of the three electron−ion distance regions outlined in Figure 1b−d; note that for the Na^+−O $g(r)$'s shown on the left, the y-axis scale is different in each panel. The e^-−O and Na^+−H $g(r)$'s shown in Figure S3 in the Supporting Information closely follow the e^-−H and Na^+−O $g(r)$'s in Figure 2 because the same water molecules are involved. The radial distribution functions in parts e and f of Figure 2 show that at larger e^-−Na^+ distances (region III), the structures of the water around both the electron and sodium cation are similar to those of the isolated species for each model, which are shown in panels g and h, respectively. This indicates that there is relatively little interaction between these species and their first solvation shells at separation distances farther than ∼4 Å, consistent with the flat PMF in this region.

Figure 3 shows integration of the first-shell peaks in $g(r)$'s shown in Figure 2 (up to 3.0 Å for water oxygens around Na^+ and 3.5 and 2.5 Å for water O atoms and H atoms around the hydrated electron, respectively) to obtain the number of first-shell waters around each species. In region III, we see that there are roughly 3.7 waters in the hydrated electron's first solvation shell (panel b) and roughly 5.3 waters in the sodium cation's first solvation shell (panel a), which is only slightly less than the number of first-shell waters around the isolated species (4.5 and 5.6 waters, respectively, black bars). In summary, at the asymptotic region (region III), both the Na^+ and the electron are separated enough to be essentially independent.

When the hydrated electron forms its stable contact pair with the sodium cation, region II, parts c and d of Figure 2 show significant changes in the solvation structures of each species, as well as sharp differences between the different ion−water simulation models. The most obvious change is a significant decrease in the height of the first-shell solvation peak for Na^+, compared with panel e at region III: Figure 3a shows that there are on average two fewer waters in the cation's first solvation shell in the region II contact pair than when the species are separated. This indicates that, to form a stable electron−ion contact pair, the electron needs to displace roughly two waters from the cation's first solvation shell. Similarly, even though the number of water O atoms near the electron does not change dramatically between regions III and II (Figure 3b), the number of H-bonds solvating the hydrated electron significantly decreases in region II (Figure 3c). Moreover, and a new e^--H peak appears at longer distances in region II (Figure 2d). All of this suggests that the first-shell water molecules around the electron in the contact pair are forced by cation−water interactions to orient with their H atoms pointing away from the electron.

Parts c and d of Figure 2 and Figure 3 also show that the Koneshan model has the highest number of solvating waters for both the Na^+ and the hydrated electron in region II. The Koneshan cation−water interaction parameters, summarized in Table 1, have the smallest Na^+−water distance (σ) among the three models. Thus, in this model, the cation hangs on much more tightly to its first-shell waters, as demonstrated by the sharp first peak shown in Figure 2 panel g. Thus, even though the TB e^-−water pseudopotential is highly repulsive, the

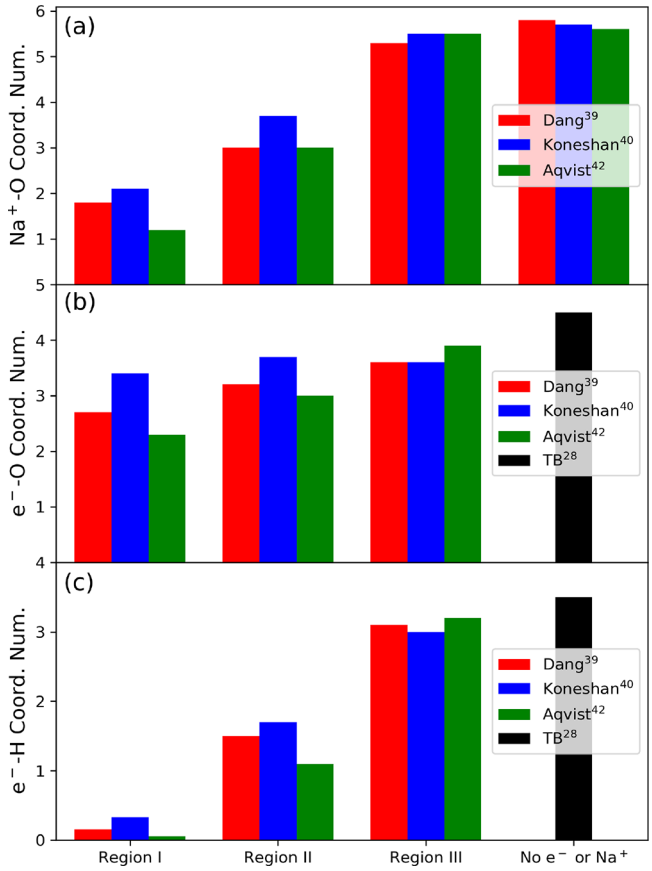

Figure 3. First-shell solvation coordination numbers of Na^+ and the hydrated electron for the three simulation models in each of the three regions defined in Figure 1 (colored bars with the same scheme as Figures 1 and 2), as well as for the isolated TB hydrated electron and aqueous Na^+ systems (black bars). The values were obtained by integrating the $g(r)$'s in Figure 2. The first shells are defined as all water O sites within 3 Å of the Na^+ and 3.5 Å of the electron's center-of-mass, and all water H sites within 2.5 Å of the electron's center-of-mass. The overall trend is similar to what is observed in the radial distribution function with decreasing coordination number as the cation−electron distance is decreased. The fact that the O and H solvation numbers around the electron change differently in the different regions indicates a change in water orientation around the electron when it is in the vicinity of the sodium cation. The Koneshan model (blue bars). with its stronger cation−water interactions, produces higher coordination of both the cation and the electron.

nearby electron is less able to displace first-shell waters from a cation described with the Koneshan LJ parameters than for cations represented by the other models. We will argue below that the increased number of waters in the electron's first shell for this model are those that are strongly bound to the sodium cation: these waters are literally forced into the electron's vicinity with an unfavorable orientation, and although they reside at a distance that is similar to the electron's natural first solvation shell, they do not help participate in solvation of the electron. This provides our first hint as to why the electron−ion PMF for the Koneshan model shows a much less stable contact pair than the other models we considered.

Finally, parts a and b of Figure 2 show that when the sodium cation is forced to reside near the center of the electron, region I, there are further changes to the local solvation structure. The TB model of the hydrated electron has a radius of gyration of 2.45 Å, which is smaller than the diameter of the Na^+ ions in all

https://doi.org/10.1021/acs.jpcb.1c08256
J. Phys. Chem. B 2021, 125, 13027−13040

Table 2. Direct Overlap (Eq 1), Radius of Gyration and Electronic Eigenvalue for Each of the Three Electron−Na^+ Simulation Models in Each of the Three Regions Defined in Figure 1

	Na^+ Direct Overlap	H_2O Direct Overlap	Radius of Gyration	Eigenvalue
Dang[39] Region I	47.17%	1.75%	2.22 Å	-3.73 eV
Dang[39] Region II	30.35%	2.15%	2.22 Å	-3.64 eV
Dang[39] Region III	2.37%	3.54%	2.42 Å	-3.03 eV
Koneshan[40] Region I	42.50%	2.12%	2.24 Å	-3.57 eV
Koneshan[40] Region II	24.10%	2.66%	2.24 Å	-3.39 eV
Koneshan[40] Region III	0.45%	3.52%	2.43 Å	-2.95 eV
Aqvist[42] Region I	50.69%	1.65%	2.21 Å	-3.79 eV
Aqvist[42] Region II	35.30%	2.02%	2.18 Å	-3.72 eV
Aqvist[42] Region III	1.24%	3.58%	2.41 Å	-2.99 eV
Hydrated e^- (no Na^+)	N/A	5.7%	2.43 Å	-3.08 eV
Gas Phase Na Atom	53.28%	N/A	2.26 Å	-4.02 eV

three models. Even though the radius of gyration of the electron shrinks to around 2.2 Å when restrained to have the sodium cation inside of it, the repulsive electron prevents water molecules from residing at the distance where the natural first solvation shell of the ion would be, leading to the drop in cation coordination seen for all three models in Figure 3a. As above, the Koneshan model (blue), with the strongest ion−water interactions, is better able to keep waters in its first solvation shell than the other models. This ion−water attraction forces water to reside inside the first natural solvation shell of the electron, effectively creating a combined species that behave as an object with no net charge due to the presence of the interior cation. The disappearance of the first peak in the electron−hydrogen $g(r)$, Figures 2b and 3c, suggests that the first-shell H atoms are oriented away from the electron, emphasizing that the system is indeed behaving more like a solvated neutral sodium atom than a cation−electron contact pair.

Overall, what the data in Figures 2 and 3 show is that there is a subtle interplay between solvation of a sodium cation and solvation of the hydrated electron when the two species approach to form a contact pair. In general, the repulsive electron displaces water from around the Na^+ to provide for a favorable electronic interaction, but the sodium cation also wants to maintain its favorable solvation environment in the water. Since Na^+ is solvated by the water O atoms, which are highly repulsive to the electron, the tighter a sodium cation hangs on to its first-shell waters, the more unfavorable the interaction between it and the hydrated electron. Because these interactions are all closely balanced, modest changes in the ion−water interactions can make relatively large changes in the solvation structure of the electron−ion contact pair.

Electronic Structure of Hydrated Electron−Na^+ Contact Pairs. Now that we have seen how the solvation structure of hydrated electron−sodium cation contact pairs changes as a function of Na^+−e^- distance and ion−water interaction model, we turn next to exploring how this solvation structure alters the electronic properties of the contact pairs. Solvated electrons are interesting objects because their properties are entirely determined by their interaction with the surrounding solvent. A solvated electron−sodium cation contact pair, however, has a behavior somewhere between that of a solvated neutral sodium atom and a solvated electron, as exemplified by previous experiments and simulations studying solvated electron−Na^+ contact pairs in liquid tetrahydrofuran (THF).[50−53] The question we explore in this section is for aqueous sodium cation−hydrated electron contact pairs: how do changes in the cation−water interactions affect the pair's electronic properties?

We begin our examination of the contact pair's electronic structure by examining how the proximity of the sodium cation to the hydrated electron's center-of-mass affects the electronic interaction of the electron with both the sodium cation and the surrounding water molecules. We characterize this by examining the direct overlap, Θ, given by

$$\Theta = \left\langle \sum_{i=1}^{n_{\text{molcs}}} 4\pi \int_0^{r_c} r_i^2 |\Psi(r_i)|^2 \, dr_i \right\rangle \quad (1)$$

where the angled brackets represent an ensemble average, Ψ is the normalized wave function of the quantum-mechanically treated electron, the sum runs over either the single sodium cation or all of the water molecules, and r_i is the distance between the electron and the appropriate classical species. The parameter r_c is set to be 1.0 Å for water, a value we have used previously to compare different hydrated electron models to each other,[30,54] and 2.0 Å for Na^+, to represent the average size of the Na 3*s* atomic orbital. The value of Θ thus gives the fraction of the electron residing on top of the centers of either the waters or the nearby sodium cation. The values of the direct overlap of the electron with both Na^+ and water for the three water−ion models at all three different regions are given in Table 2.

https://doi.org/10.1021/acs.jpcb.1c08256
J. Phys. Chem. B 2021, 125, 13027−13040

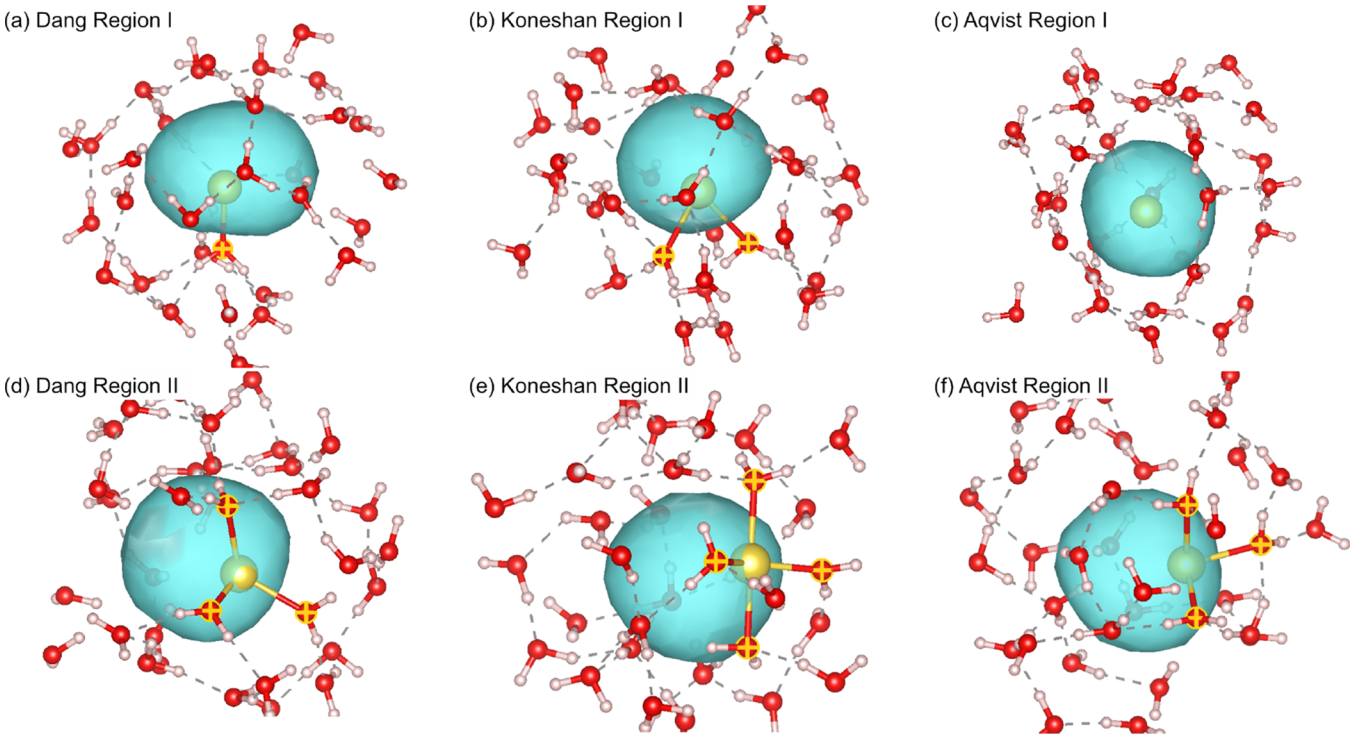

Figure 4. Representative simulation snapshots of Na^+−hydrated electron contact pairs for regions I (panels a−c) and II (panels d−f) for all three ion−water models. First-shell water O atoms within 3 Å of the Na^+ are marked with yellow crosses. The Koneshan model cation manages to keep two waters in its first solvation shell in region I and four in region II, whereas the other models have either zero or one first-shell water in region I and only three in region II. The first-shell waters that stabilize the cation are oriented so that their H atoms unfavorably point away from the electron, providing a trade-off in net solvent stabilization of the contact pair. The Aqvist model shows an almost perfect clathrate solvation structure in region I.

Table 2 shows that, in region III, the electron−water direct overlap is ∼3.5%, a little less compared with the isolated TB electron,[30] which is understandable due to the slightly decreased water−electron coordination discussed above. The electron's average eigenvalue is similar to what is observed for the bare TB electron, and the electron−Na^+ overlap in this region is essentially negligible. This indicates that at this distance, there is effectively no interaction between the electron and the sodium cation, and that we are truly in the asymptotic region.

In contrast, we see significant changes in electronic structure when the electron forms a contact pair with Na^+. In region II, the electron's direct overlap with the Na^+ dramatically increases, to about half that seen in a bare gas-phase neutral Na atom. The direct overlap of the electron with water decreases, a direct result of the structural changes that put less water in the electron's first solvation shell seen in Figure 2. One way to think about the contact pair is that the sodium cation now lies within the electron's radius of gyration, creating a direct electronic interaction, so that Na^+ occupies space where water otherwise would have resided in the electron's first solvation shell.

The contact-pair interaction between the electron and sodium cation in region II, however, is highly dependent on the model used to represent the Na^+−water interactions. The Koneshan model, with its tight cation−water interactions, has the lowest electron−Na^+ overlap and highest electron−water overlap. This is because the cation in this model is holding more tightly onto its own first-shell waters, which in turn repel the electron from the region around the cation. We also believe that this is the reason the PMF minimum for this model is observed at the longest ion−water distance; pulling Na^+ closer to the electron's center becomes more unfavorable as additional waters are forced to enter the electron's cavity. The electron's contact-pair eigenvalue is also significantly higher (less bound) for the Koneshan model compared to the other two, both because there is less stabilization from the sodium cation and because the electron has a more unfavorable solvation structure. All of this explains why this model has a much shallower PMF for the contact pair seen in Figure 1.

In region I, as the sodium cation is forced to sit close to the electron center-of-mass, the direct overlap of the electron on the Na^+ is 40−50%, consistent with the idea that the system is approaching the behavior of a solvated neutral Na atom, which in the gas phase has a direct overlap of 53%. The direct overlap of the electron with the water decreases; this is because the first-shell waters are trying to solvate a neutral object and thus are forming a clathrate-like structure, as will be discussed further below. The electronic properties in region I are also strongly model-dependent, with the Koneshan model showing the least Na^+ overlap. Again, this is because the Koneshan Na^+ strongly attracts water, which in turn repels the electron, also leading to the highest eigenvalue of the three models. This explains why the Koneshan PMF shows the most unfavorable free energy in this region, reaching ∼14 k_BT as Na^+ is forced into the electron's center.

The structural and electronic changes that a hydrated electron undergoes in the vicinity of a sodium cation are visualized in Figure 4, which shows representative snapshots of the system in regions I and II for all three models. Oxygen atoms are marked with yellow crosses if they are within the first solvation shell (≲3 Å) of the sodium cation. Not surprisingly,

https://doi.org/10.1021/acs.jpcb.1c08256
J. Phys. Chem. B 2021, 125, 13027−13040

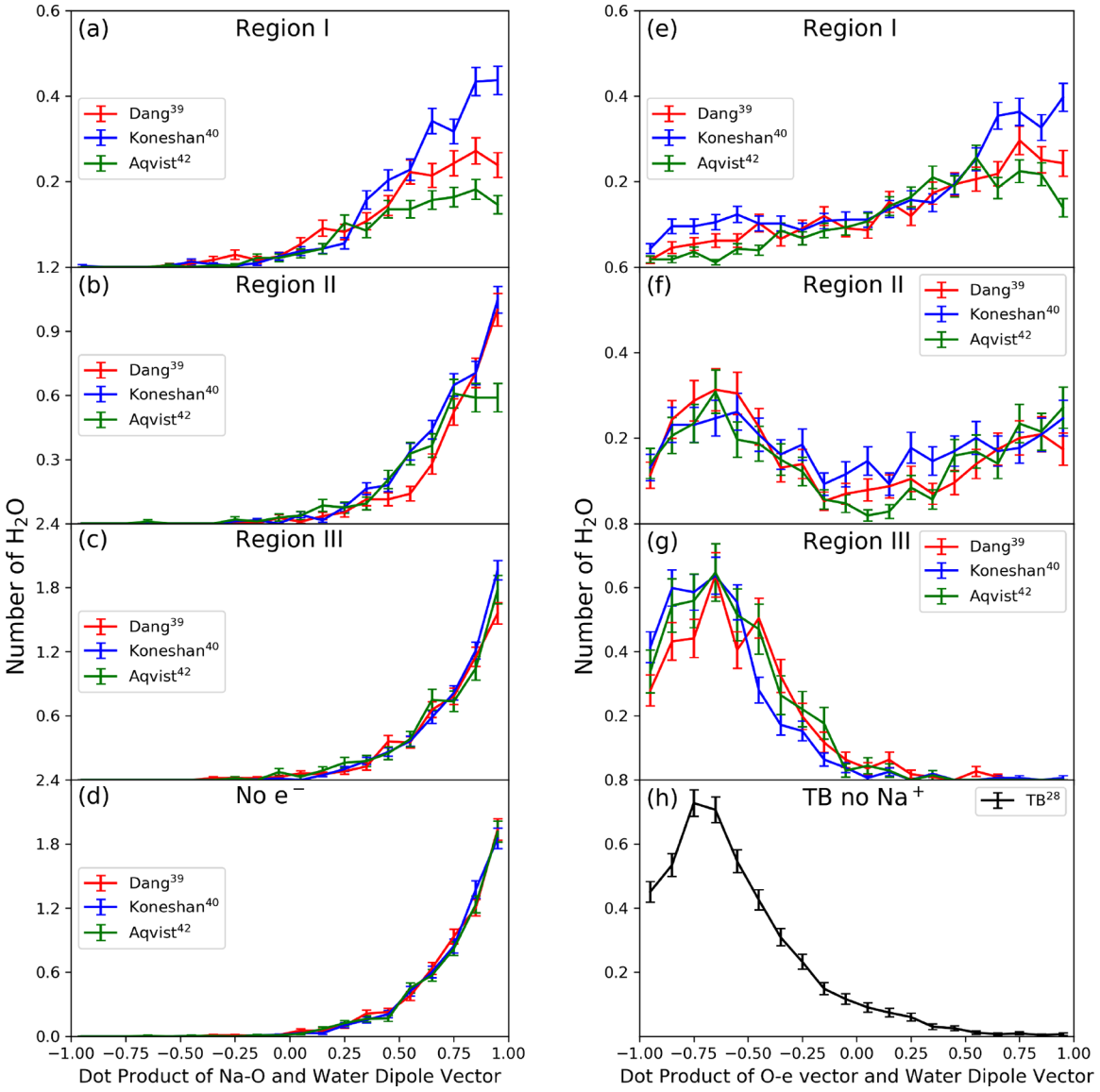

Figure 5. Distribution of dot products of the Na^+−O vector and water dipole vector for waters with O atoms that are in the first solvation shell of Na^+ (panels a−c) for each of the three contact pair models in each of the three regions defined in Figure 1. Panels e−g show the same distributions for first-shell waters relative to the electron's center of mass. Panels d and h show the same distributions for isolated Na^+ and TB hydrated electrons, respectively. The dot product is defined as 1.0 when the negative end of the water dipole points directly toward the species, and −1.0 when the positive end of the dipole points toward the species. With this definition, when water H bonds are oriented toward the electron, the dot product is around −0.75. Clearly, the water orientation around Na^+ does not change significantly between the three regions, while that around the hydrated electron undergoes a dramatic change when present in a contact pair.

all such O atoms are on waters that have their H atoms pointing away from the cation. There are few of these waters in region I, and the clathrate solvation structure of what is essentially a neutral Na atom is evident: the closest water H bonds are preferentially directed around the cation/electron pair rather than toward or away from either species. In both regions I and II, it can be seen that the Koneshan model has a higher cation−water coordination number (cf. Figure 3), forcing those waters to be in an unfavorable location and orientation with respect to the electron. Thus, the dramatic difference in contact pair stability for the different solvation models is a result of a slight shift in the balance of competing interactions between cation solvation, electron solvation and the direct cation−electron interaction.

To better understand how solvation of the Na^+ competes with solvation of the electron in the electron−ion contact pair, we examine the orientational distribution of the water molecules in the first solvation shells of both the electron and the cation in Figure 5. These distributions were constructed by taking the dot product of the water dipole vector with the vector connecting first-shell water O atoms with either the sodium cation (left column of Figure 5) or the hydrated electron center-of-mass (right column of Figure 5). The bottom two panels show that the water O atoms point directly at the sodium cation when no electron is present (dot product of 1.0), and that water H bonds point toward the center of an isolated TB hydrated electron (dot product of ∼ −0.75). Parts c and g of Figures 5 show that, in region III, the orientational distributions of the waters around each species

https://doi.org/10.1021/acs.jpcb.1c08256
J. Phys. Chem. B 2021, 125, 13027−13040

are the same as when they are isolated, which is again consistent with the idea that by the time the species are separated by ∼5 Å, they are essentially independent.

In contrast, when the contact pair forms in region II, panels b and f of Figure 5 show that the water orientational distribution around the Na^+ remains essentially unchanged, but the orientation of the waters around the hydrated electron changes significantly: there are now a significant number of waters pointing the "wrong way", with their O atoms toward the electron's center of mass. This indicates that contact pair formation is primarily a trade-off between losing favorable solvation of the electron and getting the maximal possible electron−cation interaction.

The most striking difference between the different cation−water models appears in region I, where the Koneshan model maintains the bare ion water orientational distribution to a much greater extent than either the Dang or Aqvist models. Thus, not only does the slight change in classical LJ parameters change the coordination number of the sodium cation, but it also helps to lock in the water orientation in the first solvation shell. The extra degree of favorable solvation of the cation in the Koneshan model, however, comes at a price: the waters around the cation are clearly oriented unfavorably for the hydrated electron, and also hinder electron−cation overlap, so that the Koneshan model creates the least stable species in region I. These changes in relative solvation also affect the electron's radius of gyration and eigenenergy, which are plotted as a function of electron−cation distance for each of the three models in Figure S4 in the Supporting Information.

Calculated Spectroscopy of Hydrated Electron−Na^+ Contact Pairs. The calculations presented so far allow us to make sense of why subtle changes in the water−ion LJ parameters lead to such large changes in the stability of electron−ion contact pairs. This leads to the question of which of these models, if any, allow for the most direct connection to experiment. As mentioned in the Introduction, experiments have shown that when hydrated electrons are created in aqueous electrolytes, the spectrum of the electron blue shifts.[14] The magnitude of the observed blue shift depends on the salt concentration, and also the identities of the cation and anion, suggesting that the spectral shift reflects an interplay between solvation of the electron, solvation of the cation, and the way that cation−anion contact pairs affect the formation of cation−electron contact pairs.

In previous work, Boutin and co-workers attempted to theoretically reproduce the concentration dependence of the electron's spectral shifts in the presence of salts via MQC simulation. These workers studied the electron's interaction with a single sodium cation and assumed that the concentration dependence could be accounted for by adjusting the distance between the cation and electron as the inverse cube root of the salt concentration.[17] They found that the electron's spectrum did blue shift in a manner that was inversely related to the electron−cation distance. They also saw that as the cation was brought close to the electron, a new shoulder appeared on the blue side of the electron's spectrum that was not observed experimentally.

To better understand how different choices of the ion−water interaction affect the spectroscopy of cation−electron contact pairs, we calculated the absorption spectrum for all three models in the three different regions summarized in Figure 1. The absorption spectrum was generated in the inhomogeneous limit by calculating the oscillator strength between the ground and the three lowest electronic excited states and then binning the oscillator strengths according to the energy difference between them. The resulting histograms were then convoluted with a Gaussian kernel, resulting in a final expression for the spectrum of:

$$I(E) = \left\langle \sum_{i=1}^{N} |\mu_{0,i}|^2 \Delta E_{0,i} \sqrt{\alpha/\pi}\, \exp(-\alpha(E - \Delta E_{0,i})^2) \right\rangle \tag{2}$$

where the angled brackets indicate an ensemble average and the Gaussian width α was chosen to be 50 eV^{-2} following previous work from our group.[55] For each model and region, a minimum of 100 uncorrelated configurations were used to generate the spectra. The normalized absorption spectra calculated this way are shown in Figure 6.

Figure 6c shows that, in region III, the calculated spectra of the different model contact pairs are effectively the same as that of an isolated TB hydrated electron, consistent with the idea that the two species are essentially independent in this region. In region II, Figure 6b shows that the calculated spectra are all significantly blue-shifted; as with the prior work of Boutin and co-workers,[17] the calculated blue shifts are an order of magnitude larger than those seen experimentally.[14] Surprisingly, Figure 6c shows that the magnitude of the blue shift is not monotonic with the cation−electron distance: for the Dang model, there is no additional blue shift between regions I and II, but for the Aqvist model, the spectrum in region I is actually red-shifted from that in region II. This trend is consistent with what is observed for the electron's radius of gyration, seen in Figure S4 in the Supporting Information, and likely reflects a shift in the energy of the excited state from that of a hydrated electron to something that more resembles the 3p state of a neutral Na atom.

The spectra shown in Figure 6 are associated with the three different regions of the PMFs, and thus they do not provide a direct way to compare to what would be measured experimentally. To better compare the simulations to experiment, we averaged the calculated absorption spectra from all of the simulated umbrella windows for each model and weighted them by the Boltzmann factor using the free energies from the calculated PMFs. These Boltzmann-weighted spectra are shown in Figure 7a.

Even with this Boltzmann-weighted spectrum, a direct comparison with the experiment requires some finesse because the effective cation concentration is not well-defined for a single-cation system. In previous work, Boutin et al. attempted to use the inverse cube-root of the restrained cation−electron distance as an approximation to the experimental concentration.[17] This approximation fails, however, as the calculated spectral shift turns out to be nonmonotonic with electron:cation distance (cf. Figure 6) while the experimental shift is monotonic with cation concentration.[14] For our Boltzmann-weighted calculated spectrum, we averaged all the single-distance spectrum together up to a cation:electron separation of 5 Å (averaging to distances further than this leads to almost no change in the averaged spectrum because there is little Boltzmann weight to the configurations at the longer distances). If we assume that our effective concentration is one cation in the volume of a 5-Å-radius sphere, this would correspond to an experimental concentration of 3.2 M. The experimental spectrum of the hydrated electron, both in neat water (cyan curve) and in the presence of 5 kg mol^{-1} NaCl

https://doi.org/10.1021/acs.jpcb.1c08256
J. Phys. Chem. B 2021, 125, 13027−13040

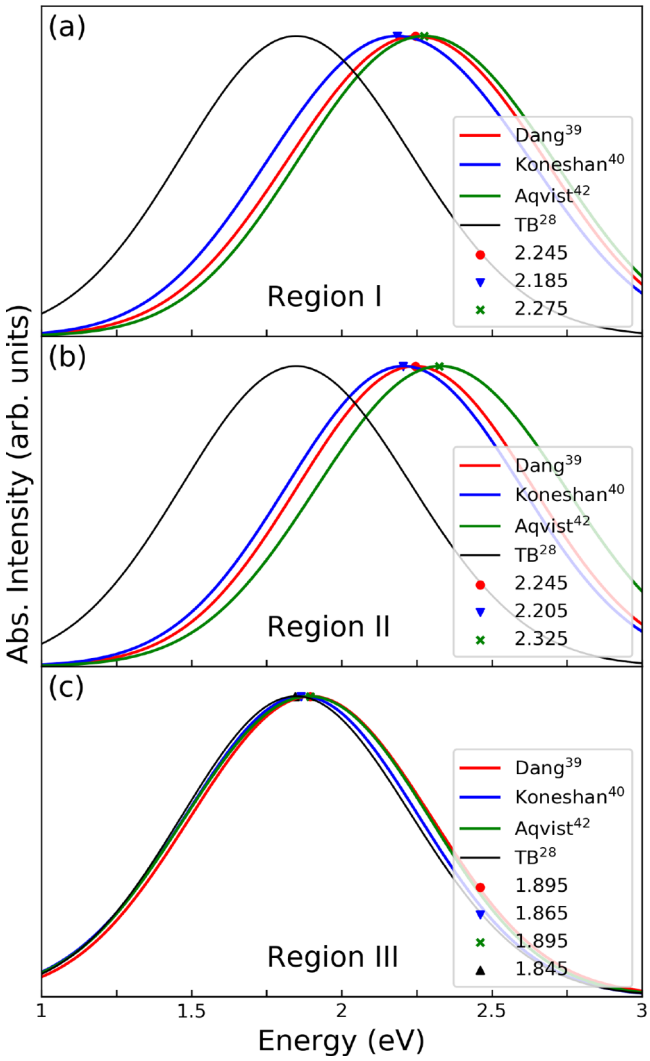

Figure 6. Absorption spectrum of each hydrated electron−cation contact pair model in each of the three regions described in Figure 1. Panels a−c depict the spectra in regions I, II, and III, respectively. The different colors correspond to the different models, as in the previous figures, and the colored labels indicate the position of the maximum of each spectrum in eV. All three models predict a spectral blue-shift of the contact pair relative to the bare hydrated electron that is an order of magnitude larger than what is observed experimentally. The predicted blue shift is smallest for the Koneshan model, likely due to the fact that the electron−cation overlap is reduced in this model due to the tight hydration of the cation.

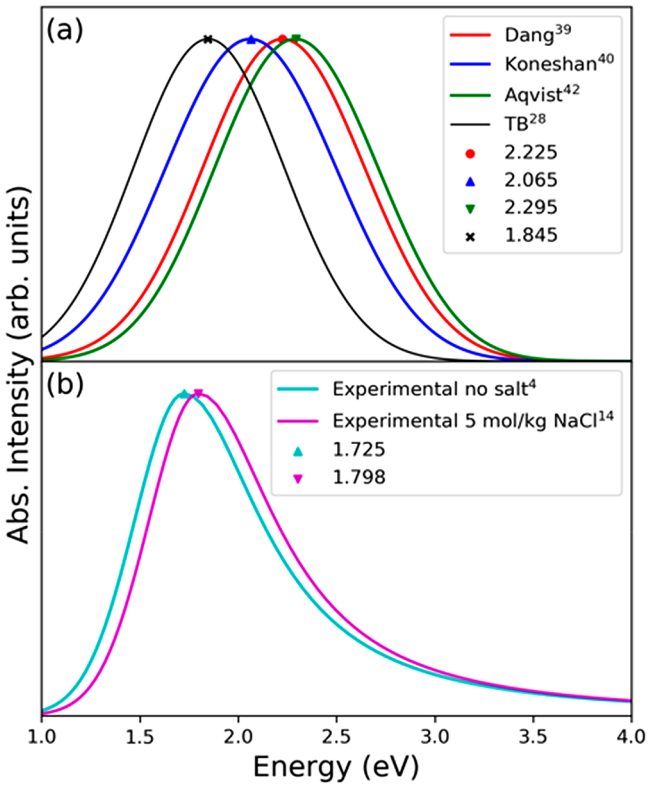

Figure 7. The absorption spectrum shown in panel a is calculated by weighing the absorption spectra from all simulation windows by the Boltzmann factor. The red, blue and green curves represent the weighed spectrum for the Dang, Koneshan and Aqvist models, respectively; the colored labels indicate the position of the maximum of each spectrum in eV. Panel b shows the experimental absorption spectra for the hydrated electron in different conditions. The cyan curve shows the hydrated electron without salts, and the magenta curve shows the hydrated electron with 5 mol kg^{-1} NaCl.

(magenta curve), are shown in Figure 7b; the spectra are reproduced using the standard Gaussian−Lorentz form (see the Supporting Information for details) with the parameters measured by Mostafavi and co-workers.[3,14] The experiments show that even at very high salt concentrations, the magnitude of the blue-shift is only 73 meV.

A comparison between the Boltzmann-averaged simulated spectra and the experimental spectrum shows that the MQC-calculated blue shift of the electron's spectrum in the presence of sodium relative to that in the absence of salt is significantly too large. Both the Dang and Aqvist models yield an averaged spectrum similar to that seen in region II, because the other regions have negligible Boltzmann weight. The Koneshan model, however, shows a smaller blue shift of the averaged spectrum compared to that in region II, because the shallower PMF for this model increases the relative Boltzmann weight of configurations at larger cation:electron separations, which have smaller spectral shifts. This makes the Koneshan weighted spectrum in somewhat better agreement with the experimental shift, although the blue shift for this model is still notably larger than the experiment. Thus, our MQC simulations fail to accurately reproduce the experimentally observed blue-shift of the hydrated electron's spectrum in the presence of salt, indicating that some factor in the MQC calculations is improperly balanced and thus does not correctly describe the nature of Na^+:e^- contact pairs in water.

Overall, the Koneshan model shows the least blue-shifted absorption spectrum, while the Aqvist model produces the largest blue-shift. This is a direct reflection of the decreased electron−cation overlap in the Koneshan model. Since none of the models produce the correct order of magnitude for the blue-shift, it is not clear if the Koneshan model is in the best agreement with experiment (i.e., that there is relatively little overlap of hydrated electrons with sodium cations in solution) or not. It is entirely possibly that our MQC model misses some of the important physics of the system; for example, the TB model of the electron, although giving a structure in reasonable agreement with ab initio calculations,[19,22,23,28] is so strongly cavity forming as to be unable to reproduce the temperature dependence of the hydrated electron's spectrum.[6] It is also possible that the electron partially occupies the water LUMOs,

https://doi.org/10.1021/acs.jpcb.1c08256
J. Phys. Chem. B 2021, 125, 13027−13040

changing the way the waters interact with the cations in a manner that is not well captured using pseudopotentials. Another factor might be that the experimental measurements occur at salt concentrations that are on the order of a few molar, so that the correct physics may involve interactions with multiple cations instead of only a single cation. Finally, we know experimentally that the anion also plays a role in the spectral blue-shift, and we plan to explore this in future work.

CONCLUSIONS

In summary, we have found that relatively modest changes in the interactions between a sodium cation and water have a large effect on the stability and properties of sodium cation:hydrated electron contact pairs. The free energy of these contact pairs and the equilibrium distance at which they prefer to reside change significantly between the different models, as evidenced by large changes in the electron-cation PMF. We argued that the differences result from the strength of the ion−water interaction: stronger ion solvation leads to poorer solvation of the electron in the contact pair and also reduces the direct interaction of the electron with the cation. This is because the solvation interactions with the cation are somewhat stronger than those with the electron, so that waters that accompany the cation are held near the electron in an unfavorable orientation. Thus, electron−cation contact pair stability arises from a delicate balance between competing effects, including electron solvation, cation solvation and cation−electron electronic interactions. Small changes in any of these interactions tip the balance, altering the nature of the electron−cation contact pairs.

We also found that despite the sensitivity of the simulated contact pair properties to the choice of ion−water interactions, all three models we explored predicted a spectral blue-shift of the contact pair that is an order of magnitude larger than that observed experimentally. This strongly suggests that the physics of the system is either not well represented by a single cation, or that quantum interactions that go beyond MQC play an important role. The fact that the experimental system shows only a relatively small spectral blue-shift ($\lesssim$100 meV shift of the electron's $\sim$ 1.7 eV absorption maximum) suggests that, on the continuum of contact-pair behavior from isolated hydrated electron to solvated neutral Na atom, the experimental system behaves more like a slightly perturbed hydrated electron than a solvated neutral atom.

All of the above results suggest that obtaining a theoretical understanding of the behavior of solvated electron in aqueous electrolytes remains a serious challenge. Describing a system with hundreds of water molecules and tens of cations and anions with *ab initio* molecular dynamics is simply out of reach computationally, and MQC simulations are clearly highly sensitive to the choice of parameters used to describe the classical part of the system and also may miss quantum aspects that are important to the physics of contact pair formation. Given that hydrated electrons often appear in solutions containing electrolytes, we believe that this remains a fruitful area for study both experimentally and theoretically.

ASSOCIATED CONTENT

Supporting Information

The Supporting Information is available free of charge at https://pubs.acs.org/doi/10.1021/acs.jpcb.1c08256.

Parameters used in the simulation, additional details of the simulations methodology, and additional data analysis including radial distribution function, radius of gyration, and absorption spectrum in the different umbrella windows (PDF)

AUTHOR INFORMATION

Corresponding Author

Benjamin J. Schwartz − *Department of Chemistry and Biochemistry, University of California, Los Angeles, Los Angeles, California 90095-1569, United States;* orcid.org/0000-0003-3257-9152; Email: schwartz@chem.ucla.edu

Authors

Sanghyun J. Park − *Department of Chemistry and Biochemistry, University of California, Los Angeles, Los Angeles, California 90095-1569, United States*

Wilberth A. Narvaez − *Department of Chemistry and Biochemistry, University of California, Los Angeles, Los Angeles, California 90095-1569, United States*

Complete contact information is available at: https://pubs.acs.org/10.1021/acs.jpcb.1c08256

Notes

The authors declare no competing financial interest.

ACKNOWLEDGMENTS

This work was supported by the National Science Foundation under Grant Number CHE-1856050. Computational resources were provided by the UCLA Institute for Digital Research and Education.

REFERENCES

(1) Garrett, B. C.; Dixon, D. A.; Camaioni, D. M.; Chipman, D. M.; Johnson, M. A.; Jonah, C. D.; Kimmel, G. A.; Miller, J. H.; Rescigno, T. N.; Rossky, P. J.; et al. Role of water in electron-initiated processes and radical chemistry: Issues and scientific advances. *Chem. Rev.* **2005**, *105*, 355−390.

(2) Davies, M. J.; Truscott, R. J. Photo-oxidation of proteins and its role in cataractogenesis. *J. Photochem. Photobiol., B* **2001**, *63*, 114−125.

(3) Jou, F.-Y.; Freeman, G. R. Temperature and isotope effects on the shape of the optical absorption spectrum of solvated electrons in water. *J. Phys. Chem.* **1979**, *83*, 2383−2387.

(4) Bartels, D. M.; Takahashi, K.; Cline, J. A.; Marin, T. W.; Jonah, C. D. Pulse radiolysis of supercritical water. 3. Spectrum and thermodynamics of the hydrated electron. *J. Phys. Chem. A* **2005**, *109*, 1299−1307.

(5) Du, Y.; Price, E.; Bartels, D. M. Solvated electron spectrum in supercooled water and ice. *Chem. Phys. Lett.* **2007**, *438*, 234−237.

(6) Casey, J. R.; Larsen, R. E.; Schwartz, B. J. Resonance Raman and temperature-dependent electronic absorption spectra of cavity and noncavity models of the hydrated electron. *Proc. Natl. Acad. Sci. U. S. A.* **2013**, *110*, 2712−2717.

(7) Zho, C.-C.; Farr, E. P.; Glover, W. J.; Schwartz, B. J. Temperature dependence of the hydrated electron's excited-state relaxation. I. Simulation predictions of resonance Raman and pump-probe transient absorption spectra of cavity and non-cavity models. *J. Chem. Phys.* **2017**, *147*, 074503.

(8) Schlick, S.; Narayana, P.; Kevan, L. ESR line shape studies of trapped electrons in γ-irradiated 17O enriched 10 M NaOH alkaline ice glass: Model for the geometrical structure of the trapped electron. *J. Chem. Phys.* **1976**, *64*, 3153−3160.

(9) Fessenden, R. W.; Verma, N. Time resolved electron spin resonance spectroscopy. III. Electron spin resonance emission from

the hydrated electron. Possible evidence for reaction to the triplet state. *J. Am. Chem. Soc.* **1976**, *98*, 243−244.
(10) Shiraishi, H.; Ishigure, K.; Morokuma, K. An ESR study on solvated electrons in water and alcohols: difference in the g factor and related analysis of the electronic state by MO calculation. *J. Chem. Phys.* **1988**, *88*, 4637−4649.
(11) Janik, I.; Lisovskaya, A.; Bartels, D. M. Partial Molar Volume of the Hydrated Electron. *J. Phys. Chem. Lett.* **2019**, *10*, 2220−2226.
(12) Borsarelli, C. D.; Bertolotti, S. G.; Previtali, C. M. Thermodynamic changes associated with the formation of the hydrated electron after photoionization of inorganic anions: a time-resolved photoacoustic study. *Photochemical & Photobiological Sciences* **2003**, *2*, 791−795.
(13) Hare, P. M.; Price, E. A.; Stanisky, C. M.; Janik, I.; Bartels, D. M. Solvated electron extinction coefficient and oscillator strength in high temperature water. *J. Phys. Chem. A* **2010**, *114*, 1766−1775.
(14) Bonin, J.; Lampre, I.; Mostafavi, M. Absorption spectrum of the hydrated electron paired with nonreactive metal cations. *Radiat. Phys. Chem.* **2005**, *74*, 288−296.
(15) Kumagai, Y.; Lin, M.; Lampre, I.; Mostafavi, M.; Muroya, Y.; Katsumura, Y. Temperature effect on the absorption spectrum of the hydrated electron paired with a metallic cation in deuterated water. *Radiat. Phys. Chem.* **2008**, *77*, 1198−1202.
(16) Spezia, R.; Nicolas, C.; Archirel, P.; Boutin, A. Molecular dynamics simulations of the Ag+ or Na+ cation with an excess electron in bulk water. *J. Chem. Phys.* **2004**, *120*, 5261−5268.
(17) Coudert, F.-X.; Archirel, P.; Boutin, A. Molecular Dynamics Simulations of Electron- Alkali Cation Pairs in Bulk Water. *J. Phys. Chem. B* **2006**, *110*, 607−615.
(18) Herbert, J. M.; Jacobson, L. D. Structure of the aqueous electron: Assessment of one-electron pseudopotential models in comparison to experimental data and time-dependent density functional theory. *J. Phys. Chem. A* **2011**, *115*, 14470−14483.
(19) Uhlig, F.; Marsalek, O.; Jungwirth, P. Unraveling the complex nature of the hydrated electron. *J. Phys. Chem. Lett.* **2012**, *3*, 3071−3075.
(20) Uhlig, F.; Herbert, J. M.; Coons, M. P.; Jungwirth, P. Optical spectroscopy of the bulk and interfacial hydrated electron from ab initio calculations. *J. Phys. Chem. A* **2014**, *118*, 7507−7515.
(21) Johnson, E. R.; Otero-De-La-Roza, A.; Dale, S. G. Extreme density-driven delocalization error for a model solvated-electron system. *J. Chem. Phys.* **2013**, *139*, 184116.
(22) Ambrosio, F.; Miceli, G.; Pasquarello, A. Electronic levels of excess electrons in liquid water. *J. Phys. Chem. Lett.* **2017**, *8*, 2055−2059.
(23) Wilhelm, J.; VandeVondele, J.; Rybkin, V. V. Dynamics of the Bulk Hydrated Electron from Many-Body Wave-Function Theory. *Angew. Chem., Int. Ed.* **2019**, *58*, 3890−3893.
(24) Dasgupta, S.; Rana, B.; Herbert, J. M. Ab initio investigation of the resonance Raman spectrum of the hydrated electron. *J. Phys. Chem. B* **2019**, *123*, 8074−8085.
(25) Tay, K. A.; Coudert, F.-X.; Boutin, A. Mechanism and kinetics of hydrated electron diffusion. *J. Chem. Phys.* **2008**, *129*, 054505.
(26) Borgis, D.; Staib, A. Quantum adiabatic umbrella sampling: The excited state free energy surface of an electron-atom pair in solution. *J. Chem. Phys.* **1996**, *104*, 4776−4783.
(27) Turi, L.; Gaigeot, M.-P.; Levy, N.; Borgis, D. Analytical investigations of an electron−water molecule pseudopotential. I. Exact calculations on a model system. *J. Chem. Phys.* **2001**, *114*, 7805−7815.
(28) Turi, L.; Borgis, D. Analytical investigations of an electron−water molecule pseudopotential. II. Development of a new pair potential and molecular dynamics simulations. *J. Chem. Phys.* **2002**, *117*, 6186−6195.
(29) Larsen, R. E.; Glover, W. J.; Schwartz, B. J. Does the hydrated electron occupy a cavity? *Science* **2010**, *329*, 65−69.
(30) Casey, J. R.; Kahros, A.; Schwartz, B. J. To be or not to be in a cavity: the hydrated electron dilemma. *J. Phys. Chem. B* **2013**, *117*, 14173−14182.
(31) Smallwood, C. J.; Larsen, R. E.; Glover, W. J.; Schwartz, B. J. A computationally efficient exact pseudopotential method. I. Analytic reformulation of the Phillips-Kleinman theory. *J. Chem. Phys.* **2006**, *125*, 074102.
(32) Glover, W. J.; Larsen, R. E.; Schwartz, B. J. The roles of electronic exchange and correlation in charge-transfer-to-solvent dynamics: Many-electron nonadiabatic mixed quantum/classical simulations of photoexcited sodium anions in the condensed phase. *J. Chem. Phys.* **2008**, *129*, 164505.
(33) Durand, P.; Barthelat, J.-C. A theoretical method to determine atomic pseudopotentials for electronic structure calculations of molecules and solids. *Theoretica Chimica Acta* **1975**, *38*, 283−302.
(34) Glover, W. J.; Casey, J. R.; Schwartz, B. J. Free energies of quantum particles: The coupled-perturbed quantum umbrella sampling method. *J. Chem. Theory Comput.* **2014**, *10*, 4661−4671.
(35) Toukan, K.; Rahman, A. Molecular-dynamics study of atomic motions in water. *Phys. Rev. B: Condens. Matter Mater. Phys.* **1985**, *31*, 2643.
(36) Verlet, L. Computer" experiments" on classical fluids. I. Thermodynamical properties of Lennard-Jones molecules. *Phys. Rev.* **1967**, *159*, 98.
(37) Feynman, R. P. Forces in molecules. *Phys. Rev.* **1939**, *56*, 340.
(38) Martyna, G. J.; Klein, M. L.; Tuckerman, M. Nosé−Hoover chains: The canonical ensemble via continuous dynamics. *J. Chem. Phys.* **1992**, *97*, 2635−2643.
(39) Dang, L. X.; Smith, D. E. Molecular dynamics simulations of aqueous ionic clusters using polarizable water. *J. Chem. Phys.* **1993**, *99*, 6950−6956.
(40) Koneshan, S.; Rasaiah, J. C. Computer simulation studies of aqueous sodium chloride solutions at 298 and 683 K. *J. Chem. Phys.* **2000**, *113*, 8125−8137.
(41) Pettitt, B. M.; Rossky, P. J. Alkali halides in water: Ion−solvent correlations and ion−ion potentials of mean force at infinite dilution. *J. Chem. Phys.* **1986**, *84*, 5836−5844.
(42) Aqvist, J. Ion-water interaction potentials derived from free energy perturbation simulations. *J. Phys. Chem.* **1990**, *94*, 8021−8024.
(43) Casey, J. R.; Schwartz, B. J.; Glover, W. J. Free energies of cavity and noncavity hydrated electrons near the instantaneous air/water interface. *J. Phys. Chem. Lett.* **2016**, *7*, 3192−3198.
(44) Glover, W. J.; Schwartz, B. J. The fluxional nature of the hydrated electron: energy and entropy contributions to aqueous electron free energies. *J. Chem. Theory Comput.* **2020**, *16*, 1263−1270.
(45) Shirts, M. R.; Chodera, J. D. Statistically optimal analysis of samples from multiple equilibrium states. *J. Chem. Phys.* **2008**, *129*, 124105.
(46) Sauer, M. C.; Shkrob, I. A.; Lian, R.; Crowell, R. A.; Bartels, D. M.; Chen, X.; Suffern, D.; Bradforth, S. E. Electron photodetachment from aqueous anions. 2. Ionic strength effect on geminate recombination dynamics and quantum yield for hydrated electron. *J. Phys. Chem. A* **2004**, *108*, 10414−10425.
(47) Renou, F.; Mostafavi, M.; Archirel, P.; Bonazzola, L.; Pernot, P. Solvated electron pairing with earth alkaline metals in THF. 1. Formation and structure of the pair with divalent Magnesium. *J. Phys. Chem. A* **2003**, *107*, 1506−1516.
(48) Rutherford, A.; Duffy, D. The effect of electron−ion interactions on radiation damage simulations. *J. Phys.: Condens. Matter* **2007**, *19*, 496201.
(49) Savéant, J.-M. Effect of ion pairing on the mechanism and rate of electron transfer. Electrochemical aspects. *J. Phys. Chem. B* **2001**, *105*, 8995−9001.
(50) Cavanagh, M. C.; Larsen, R. E.; Schwartz, B. J. Watching Na Atoms Solvate into (Na+, e-) Contact Pairs: Untangling the Ultrafast Charge-Transfer-to-Solvent Dynamics of Na-in Tetrahydrofuran (THF). *J. Phys. Chem. A* **2007**, *111*, 5144−5157.
(51) Glover, W. J.; Larsen, R. E.; Schwartz, B. J. First principles multielectron mixed quantum/classical simulations in the condensed phase. II. The charge-transfer-to-solvent states of sodium anions in liquid tetrahydrofuran. *J. Chem. Phys.* **2010**, *132*, 144102.

https://doi.org/10.1021/acs.jpcb.1c08256
J. Phys. Chem. B 2021, 125, 13027−13040

(52) Widmer, D. R.; Schwartz, B. J. The role of the solvent in the condensed-phase dynamics and identity of chemical bonds: The case of the sodium dimer cation in THF. *J. Phys. Chem. B* **2020**, *124*, 6603−6616.
(53) Vong, A.; Widmer, D. R.; Schwartz, B. J. Nonequilibrium Solvent Effects during Photodissociation in Liquids: Dynamical Energy Surfaces, Caging, and Chemical Identity. *J. Phys. Chem. Lett.* **2020**, *11*, 9230−9238.
(54) Park, S. J.; Schwartz, B. J. Evaluating Simple Ab Initio Models of the Hydrated Electron: The Role of Dynamical Fluctuations. *J. Phys. Chem. B* **2020**, *124*, 9592−9603.
(55) Glover, W. J.; Schwartz, B. J. Short-range electron correlation stabilizes noncavity solvation of the hydrated electron. *J. Chem. Theory Comput.* **2016**, *12*, 5117−5131.

https://doi.org/10.1021/acs.jpcb.1c08256
J. Phys. Chem. B 2021, 125, 13027−13040